Published in final edited form as:
Chem Res Toxicol. 2010 November 15; 23(11): 1815–1823. doi:10.1021/tx100260e.

Glutathione Complex Formation with Mercury(II) in Aqueous Solution at Physiological pH

Vicky Mah and **Farideh Jalilehvand**
Department of Chemistry, University of Calgary, 2500 University Dr. N. W. Calgary, AB, T2N 1N4, Canada

Abstract

The mercury(II) complexes formed in neutral aqueous solution with glutathione (GSH, here denoted AH_3 in its tri-protonated form) were studied using Hg L_{III}-edge extended X-ray absorption fine structure (EXAFS) and ^{199}Hg NMR spectroscopy, complemented with electrospray ionization mass spectrometric (ESI-MS) analyses. The $[Hg(AH)_2]^{2-}$ complex, with the Hg-S bond distances 2.325 ± 0.01 Å in linear S-Hg-S coordination and the ^{199}Hg NMR chemical shift −984 ppm, dominates except at high excess of glutathione. In a series of solutions with $C_{Hg(II)}$ ~17 mM and GSH/Hg(II) mole ratios rising from 2.4 to 11.8, the gradually increasing mean Hg-S bond distance corresponds to an increasing amount of the $[Hg(AH)_3]^{4-}$ complex. ESI-MS peaks appear at $-m/z$ values of 1208 and 1230 corresponding to the $[Na_4Hg(AH)_2(A)]^-$ and $[Na_5Hg(AH)(A)_2]^-$ species, respectively. In another series of solutions at pH = 7.0 with $C_{Hg(II)}$ ~50 mM and GSH/Hg(II) ratios from 2.0 to 10.0, the Hg L_{III}-edge EXAFS and ^{199}Hg NMR spectra show that at high excess of glutathione (~0.35 mol·dm^{-3}) about ~ 70% of the total mercury(II) concentration is present as the $[Hg(AH)_3]^{4-}$ complex, with the average Hg-S bond distance 2.42 ± 0.02 Å in trigonal HgS_3 coordination. The proportions of HgS_n species, n = 2, 3 and 4, quantified by fitting linear combinations of model EXAFS oscillations to the experimental EXAFS data in our present and previous studies, were used to obtain stability constants for the $[Hg(AH)_3]^{4-}$ complex, and also for the $[Hg(A)_4]^{10-}$ complex that is present at high pH. For Hg(II) in low concentration at physiological conditions (pH = 7.4, C_{GSH} = 2.2 mM) the relative amounts in the HgS_2 species $[Hg(AH)_2]^{2-}$, $[Hg(AH)(A)]^{3-}$ and the HgS_3 complex $[Hg(AH)_3]^{4-}$ was calculated to be 95 : 2 : 3. Our results are not consistent with the formation of dimeric Hg(II)-GSH complexes proposed in a recent EXAFS study.

Keywords

Mercury(II); glutathione; structure; solution; Hg L_{III}-edge EXAFS; ESI-MS; ^{199}Hg NMR

Introduction

Human exposure to the toxic heavy metal mercury remains a major concern because of its previous and still existing use in a number of commercial and medical products. Elemental mercury (Hg^0) has been widely utilized for dental amalgams (1), and organic mercury compounds are found in fish as methyl mercury (CH_3Hg^+) (2), and in vaccine preservatives

Supporting Information Available: PCA of Hg(II)-GSH solution EXAFS **C1**–**F1** and **B2-F2**; linear combination fitting for Hg(II)-GSH solutions **B1**–**F1** and **B2-F2**; table for assignment of mass ions in the ESI-MS of solution **F1** (GSH/Hg(II) = 11.8); fraction diagrams for solutions **B1**, **B2** and **F1**, showing distribution of Hg(II)-GSH complexes *vs*. pH using adjusted stability constant for the HgS_3 complexes, together with the calculated distribution of Hg(II) species at low concentration under physiological conditions (pH 7.4, $[GSH]_{tot}$ = 2.2 mM). This material is available free of charge via the Internet at http://pubs.acs.org."

in the form of ethyl mercury ($CH_3CH_2Hg^+$). The elemental and organic forms of mercury are in part metabolized to inorganic Hg(II) species in the body (3). Mercury toxicity is known to target the central nervous system and the kidneys, although its role in neurodegenerative disorders such as multiple sclerosis, Alzheimer's and Parkinson's diseases, and autism is a controversial subject (4).

The strong affinity of mercury(II) to the cysteinyl thiol groups in proteins and peptides can be detrimental to their normal function. One of the intracellular mechanisms of protection involves the abundant tripeptide glutathione (GSH, γ-L-glutamyl-L-cysteinyl-glycine, Scheme 1), which is able to bind to heavy metals and transport them out of the cell (5). The complex formation between mercury(II) and glutathione has been well characterized by polarographic and potentiometric titrations (6–8), ^{1}H, ^{13}C and ^{199}Hg NMR (9–11), and ESI-MS (12–15). Two separate ^{13}C NMR studies showed strong binding to the cysteinyl thiolate group of GSH forming the $[Hg(AH)_2]^{2-}$ complex for aqueous solutions of GSH/Hg(II) = 2 (AH_3 denotes the tri-protonated form of glutathione) (16,17).

In their ^{13}C NMR and polarimetric investigations, Cheesman et al. showed that for solutions with C_{GSH} = 0.2 M and molar ratios of GSH/Hg(II) ≥ 3 at pH ~ 7, a three-coordinated $[Hg(AH)_3]^{4-}$ complex forms with an estimated lifetime of 1.4×10^{-4} s (18,19). They discussed the high lability of Hg(II) in biological systems, exchanging between sulfhydryl groups of enzymes and other molecules, and proposed that the rapid exchange of thiol ligands between free and $Hg(thiol)_2$ forms proceeds via a mechanism involving $Hg(thiol)_3$ complexes. They concluded that considering the ubiquity of glutathione in cellular systems those reactions play a major role in the mobility of Hg(II) in biological systems (18).

In a recent Hg L_{III}-edge EXAFS study we showed that the $[Hg(GS)(GSH)]ClO_4$ compound, which precipitates from acidic mercury(II)–glutathione solutions (pH ~ 2.0), has linear S-Hg-S coordination geometry with a mean Hg–S distance of 2.33 ± 0.01 Å, and a Raman band at 331 cm^{-1} for the symmetric stretching ν(S–Hg–S). Additionally, the $[HgA_2]^{4-}$ complex was characterized in alkaline solutions at pH = 10.5 ($C_{Hg(II)}$ ~18 mM, C_{GSH} = 40 mM) with the Hg-S distance 2.32 ± 0.01 Å and the ^{199}Hg chemical shift −961 ppm. For the higher complexes $[HgA_3]^{7-}$ and $[HgA_4]^{10-}$, which formed at large excess of GSH, C_{GSH} ≥ 160 mM, the mean Hg-S bond distances 2.42 ± 0.02 Å and 2.52 ± 0.02 Å, respectively, were obtained (20).

To gain a better understanding of the speciation and structures of the Hg(II)-GSH complexes as a continuation of our studies of mercury(II) complexes to bio-relevant ligands (20–22), and to provide a basis for detailed studies of the reaction mechanisms for the exchange of thiol-containing ligands in biological systems, we have characterized the $[Hg(AH)_2]^{2-}$ and $[Hg(AH)_3]^{4-}$ complexes formed at near physiological pH (~7.0) in aqueous solution, combining Hg L_{III}-edge XAS and ^{199}Hg NMR spectroscopic techniques with ESI-MS. To evaluate the effect of mercury(II) and glutathione concentrations on the Hg(II) speciation, two series of solutions were prepared with different mercury(II) concentration ($C_{Hg(II)}$ ~17 mM and 50 mM) with molar ratios of GSH/Hg(II) ranging from ~2 to ~12. The higher mercury(II) concentration (50 mM) made ^{199}Hg NMR measurements possible, as complement to the EXAFS spectra. The relative amounts of HgS_2 and HgS_3 species in the form of $[Hg(AH)_2]^{2-}$ and $[Hg(AH)_3]^{4-}$ complexes in neutral aqueous solution were obtained, which allowed the free GSH concentration at pH 7.0, $[AH_2^-]$, to be derived as: $[AH_2^-] = C_{GSH} - 2[Hg(AH)_2]^{2-} - 3[Hg(AH)_3]^{4-}$.

Experimental

Sample preparation

Glutathione, sodium hydroxide and $Hg(ClO_4)_2 \cdot \sim 3.26H_2O$ were purchased from Sigma-Aldrich and used without further purification. An acidic stock solution with $C_{Hg(II)}$ = 0.17 M was prepared in ~ 0.5 M $HClO_4$, where the total Hg(II) concentration was measured by the inductively coupled plasma (ICP) technique. The Hg(II)-GSH solutions were prepared in degassed distilled water under inert Ar atmosphere, and their pH was measured with a Corning Semi-Micro electrode calibrated with standard buffers. Our attempts to crystallize complexes of Hg(II)-GSH failed due to sample decomposition.

The series of mercury(II)-GSH solutions **A1**–**F1** containing $C_{Hg(II)}$ ~17 mM was synthesized by dissolving glutathione (0.2–1 mmol) in ~3.5 mL O_2-free water (pH 2.7–2.8), followed by adding 0.5 mL of the stock Hg(II) solution (0.085 mmol Hg^{2+}). The pH decreased to < 2.0 and a white precipitate formed that dissolved with further stirring. Sodium hydroxide solution (2.0 M) was added dropwise to adjust the solution pH to 7.0. Six solutions with GSH/Hg(II) mole ratios of 2.4 (**A1**), 3.5 (**B1**), 4.7 (**C1**), 5.9 (**D1**), 9.4 (**E1**) and 11.8 (**F1**) were prepared with a final volume of 5.0 mL and pH = 7.0 (Table 1). A similar procedure was used to prepare a series of solutions with total $C_{Hg(II)}$ ~50 mM (1.5 mL stock solution) containing 10 % v/v D_2O, and with GSH/Hg(II) mole ratios of 2.0 (**A2**), 3.0 (**B2**), 4.0 (**C2**), 5.0 (**D2**), 8.0 (**E2**), and 10.0 (**F2**). The ^{199}Hg NMR spectra of solutions **A1** and **B1** were measured after addition of 10 % D_2O, reducing their concentration to $C_{Hg(II)}$ ~15 mM.

Mass spectrometry

Mass spectra were collected in negative ion mode by direct infusion of solution **F1** into the electrospray ionization (ESI) source of a Bruker Esquire 3000 mass spectrometer using a continuous injection flow rate of 0.06 mL/min. The drying gas temperature was 300 °C, with a 4 L/min flow rate. The capillary voltage was set at ~3.1 kV, the skimmer voltage was −47.5 V. The mass spectrum of the most concentrated solution **F2** could not be measured for technical reasons (contamination of the sample path in the instrument).

Nuclear Magnetic Resonance Spectroscopy

^{199}Hg NMR spectra were collected at a resonance frequency of 53.76 MHz using a Bruker AMX 300 spectrometer equipped with a 10 mm broadband probe (BB10) for the Hg(II)-GSH solutions **A1** and **B1** (diluted to $C_{Hg(II)}$ ~15 mM after adding 10 % D_2O), and **A2** – **F2** (containing 10 % D_2O and $C_{Hg(II)}$ ~50 mM). The ^{199}Hg chemical shift was externally calibrated relative to a saturated $HgCl_2$ standard solution in D_2O, resonating at −1550 ppm relative to the $Hg(CH_3)_2$ resonance at 0 ppm (20–23). NMR data were acquired using a 90° pulse, a sweep width of 59.2 kHz, and 32 K data points. A 1 s delay was used between scans, and 47000–186000 scans were collected. Spectra were processed using exponential line broadening: 10 % of $v_{1/2}$ (25 – 250 Hz).

X-ray Absorption Spectroscopy Data Collection

Hg L_{III}-edge X-ray absorption spectra, averaging 3 to 4 scans for each sample, were collected on beamline 7-3 at the Stanford Synchrotron Radiation Lightsource (SSRL) under dedicated conditions (3 GeV, 85–100 mA). The ion chambers I_0 (monitoring the incident beam) and I_1 (after the sample) were filled with N_2 gas for transmission measurements at ambient temperature, where each Hg(II)-GSH solution was held in a 10 mm (**A1** – **F1**) or 5 mm (**A2** – **F2**) Teflon spacer with 5 μm polypropylene windows. Higher order harmonics were rejected by a rhodium coated mirror on the fully tuned beam. To calibrate the energy of

the X-rays, the first inflection point of the $HgCl_2$ standard, measured simultaneously between I_1 and I_2 (filled with Ar gas), was set to 12284.0 eV.

X-ray Absorption Spectroscopy Data Analysis

The scans for each sample were visually compared using the EXAFSPAK suite of programs (24), prior to averaging. The EXAFS oscillation was extracted using the WinXAS 3.1 program (25), and converted to *k*-space, where $k = [(8\pi^2 m_e/h^2)(E-E_0)]^{1/2}$, using the threshold energy E_0 = 12285.0 eV. Effective amplitude, mean free path and phase shift functions were obtained by means of *ab initio* calculations with the FEFF 8.1 code (26,27), applied on the atomic coordinates of the linearly coordinated $Hg(cysteamine)_2$ complex (28), and used to simulate the theoretical EXAFS oscillations $\chi(k)$. The amplitude reduction factor, S_0^2, was fixed at 1.0, the value obtained for the EXAFS data analysis of the solid $[Hg(GS)(GSH)]ClO_4$ compound (20). Further details on EXAFS data analysis can be found elsewhere (21). The estimated errors for the coordination numbers and bond distances obtained from least squares curve-fitting of the EXAFS model functions are within ± 20 % and ± 0.02 Å, respectively.

Principal component analysis (PCA) implemented in the EXAFSPAK program, was applied to the k^3-weighted EXAFS spectra of solutions **C1** – **F1** and **B2** – **F2** over the range of 3.9–11.9 $Å^{-1}$, and indicated the presence of two major components in all these solutions (Figure S-1 and Table S-1). To quantify the relative proportion of the $[Hg(AH)_2]^{2-}$ and $[Hg(AH)_3]^{4-}$ complexes, linear combinations of the EXAFS model oscillations representing the $[Hg(AH)_2]^{2-}$ and $[Hg(AH)_3]^{4-}$ species, respectively, were fitted to the experimental EXAFS spectra for solutions **C1** – **F1** and **B2** – **F2**, using DATFIT in the EXAFSPAK suite of programs (Figures S-2 and S-3) (24). The EXAFS oscillation derived from the model fitting for solutions **A1** and **A2** represented the $[Hg(AH)_2]^{2-}$ species (Tables 2 and 3). The EXAFS oscillation for the $[Hg(AH)_3]^{4-}$ complex was simulated according to the procedure described previously (20).

Results

^{199}Hg NMR spectroscopy

The ^{199}Hg NMR chemical shifts for HgS_2, HgS_3 and HgS_4 coordination environments span over a wide range, generally within −800 to −1200 ppm for HgS_2, −79 to −159 ppm for HgS_3, and −275 to −374 ppm for HgS_4, depending on the type of ligand, coordination number, and nature of the solvent (29–32). The ^{199}Hg resonance for solutions **A1**–**B1** and **A2**–**F2** (Figure 1) can therefore serve as a guideline to the Hg(II) coordination. By increasing the mercury(II) concentration to ~50 mM (solutions **A2** – **F2)**, broad ^{199}Hg NMR signals could be obtained for the entire series of solutions. The increasing deshielding of the ^{199}Hg chemical shift with higher glutathione concentration in this series corresponds to an increasing number of thiolate groups coordinated to the Hg(II) ions.

Hg L_{III}-edge X-ray absorption spectroscopy

In crystal structures the Hg-S bond distances for mercury(II) complexes with thiolate ligands typically occur within discrete ranges for HgS_2, HgS_3 and HgS_4 coordination geometries, 2.30–2.38 Å (R_{ave} = 2.34 ± 0.02 Å), 2.40–2.51 Å (R_{ave} = 2.44 ± 0.04 Å), and 2.49–2.58 Å (R_{ave} = 2.54 ± 0.02 Å), respectively (22). The mean Hg-S bond length obtained from the EXAFS curve fitting for the Hg(II)-GSH solutions thus provides another indication of the mercury(II) coordination geometry (20–22,33).

The k^3-weighted EXAFS spectra for the Hg(II)-GSH solutions **A1** – **F1** are shown in Figure 2, with the structural parameters obtained from curve fitting listed in Table 2. The

corresponding Fourier transforms (FTs) show a single peak at ~2.0 Å (without phase shift correction), attributed to the Hg-S backscattering in the first coordination shell. The peak gradually becomes smaller and broader as the GSH concentration increases.

The k^3-weighted EXAFS spectrum of solution **A1** ($C_{Hg(II)}$ ~17 mM, GSH/Hg(II) = 2.4) fitted well to a model with two Hg-S bonds at 2.325 ± 0.01 Å and two S-Hg-S multiple scattering paths (n_{leg} = 4) at 4.66 ± 0.02 Å (approximately twice the Hg-S distance), characteristic of a linear coordination geometry in the $[Hg(AH)_2]^{2-}$ complex. Solutions **B1–D1** with GSH/Hg(II) mole ratios of 3.5 – 5.9 also showed very similar EXAFS oscillations, with the mean Hg-S bond distances refined to 2.33 – 2.34 Å (Figure 2). For solutions **E1** and **F1** with large excess of glutathione (C_{GSH} ≥ 160 mM) the increase in the mean Hg-S distances, 2.35 ± 0.02 Å and 2.37 ± 0.02 Å, respectively, indicated formation of a significant amount of the $[Hg(AH)_3]^{4-}$ complex (see above).

The Hg L_{III}-edge EXAFS spectra for the series of solutions **A2** – **F2** with $C_{Hg(II)}$ ~50 mM and GSH/Hg(II) mole ratios 2.0 – 10.0 at pH = 7.0 are shown in Figure 3, with the structural parameters of the Hg(II)-GSH complexes listed in Table 3.

The EXAFS oscillations for solutions **A2** and **B2** ($C_{Hg(II)}$ ~50 mM; C_{GSH} ~ 100 – 150 mM) were modeled over the k-range 3.7 – 12.0 $Å^{-1}$ by introducing two Hg-S bonds at a distance of 2.32 – 2.34 Å and a S-Hg-S multiple scattering contribution (n_{leg} = 4) at 4.64 – 4.66 Å as expected for a linear entity, in a similar way as for solutions **A1** and **B1** ($C_{Hg(II)}$ ~17 mM, C_{GSH} ~ 40 – 60 mM). For solutions **E2** and **F2** with the highest excess of glutathione (C_{GSH} = 0.4 – 0.5 M), the average Hg-S bond length was refined to 2.39 ± 0.02 Å, intermediate to the average values for crystalline HgS_2 (R_{av} = 2.34 Å) and HgS_3 (R_{av} = 2.44 Å) compounds; see above. At intermediate GSH concentration (C_{GSH} = 0.2 – 0.25 M) in solutions **C2** – **D2** the mean Hg-S distance, 2.35–2.36 Å, is comparable to the mean Hg-S distances of 2.35–2.37 Å obtained for solutions **E1** and **F1** ($C_{Hg(II)}$ ~17 mM; C_{GSH} ~ 0.16 – 0.2 M) with a similar excess of free glutathione. In the less concentrated solutions **C1** and **D1** ($C_{Hg(II)}$ ~17 mM; C_{GSH} ~ 80 – 100 mM), the lower excess of free GSH results in lower average Hg-S coordination numbers corresponding to the slightly shorter refined average Hg-S distances, 2.33 – 2.34 Å (Table 2).

Electrospray Ion Mass Spectrometry

The presence of the *tris*-glutathionyl $[Hg(AH)_3]^{4-}$ complex in the neutral solutions was also verified by measuring the ESI mass spectrum, even though the Na^+ ion pairs with mercury(II) glutathionyl complexes with partially deprotonated $-NH_3^+$ groups in the gas phase do not represent the equilibrium state in solution. The ESI-MS for solution **F1**, with an excess of free glutathione of about 0.16 M, displayed strong peaks for ionic species with mass/charge ratios $-m/z$ of 812.7, 834.7, 856.7 and 878.7, assigned as the *bis*-glutathionyl mercury(II) complexes $[Hg(AH)(AH_2)]^-$, $[NaHg(AH)_2]^-$, $[Na_2Hg(AH)(A)]^-$, and $[Na_3Hg(A)_2]^-$, respectively (Figure 4, Table S-2). *Bis*-glutathionyl mercury(II) complexes have previously been characterized in acidic solutions by ESI-MS (12–15). In the present work, the *tris*-glutathionyl mercury(II) complexes $[Na_4Hg(AH)_2(A)]^-$ and $[Na_5Hg(AH)(A)_2]^-$ could be identified by peaks with $-m/z$ values of 1208 and 1230, respectively (Figure 4). Even though their intensities are much lower than for the signals of the *bis*-glutathionyl mercury(II) complexes, the calculated isotopic distribution closely matches the experimental one.

Discussion

The previously reported formation constants for the $[Hg(AH)_2]^{2-}$ and $[Hg(AH)_3]^{4-}$ species, log β = 40.95 and 44.18, respectively, show that a *tris*-thiolate Hg(II) complex with weaker

bonding to the $(AH)^{2-}$ groups than in $[Hg(AH)_2]^{2-}$, can form at physiological pH in excess of glutathione (8,18,19). In the present work, the structure and composition of the Hg(II)-glutathione complexes formed in solution at physiological pH have been studied by combining Hg L_{III}-edge EXAFS and ^{199}Hg NMR spectroscopy, complemented by ESI-MS.

We recently reported the ^{199}Hg chemical shift −961 ppm for the $[Hg(A)_2]^{4-}$ complex in a solution containing $C_{Hg(II)}$ ~ 18 mM and C_{GSH} ~ 40 mM at pH 10.5 (20). In the current study, solution **A1** (pH 7.0) with rather similar composition shows a ^{199}Hg NMR resonance at −984 ppm, which is within the range typical for Hg(II)-dithiolates (about −800 to −1200 ppm) (32), and can be attributed to the $[Hg(AH)_2]^{2-}$ complex. This resonance is close to the value reported previously (−993 ppm) for a solution with mole ratio GSH/Hg(II) = 2 and $C_{Hg(II)}$ = 0.25 M at pH ~ 7 (11). By increasing the Hg(II) concentration to ~ 50 mM in solution **A2** (GSH / Hg(II) = 2.0), the ^{199}Hg NMR signal shifts to −960 ppm. We therefore conclude that the $[Hg(AH)_2]^{2-}$ complex completely dominates in solutions **A1** and **A2**. From the curve-fitting analyses of their EXAFS spectra, a Hg-S bond distance of 2.325 ± 0.01 Å with a relatively small disorder parameter, σ^2 = 0.0035 ± 0.001 Å^2, emerged for the $[Hg(AH)_2]^{2-}$ species, which can be compared with the Hg-S distance 2.315 ± 0.01 Å obtained for the $[Hg(A)_2]^{4-}$ complex with deprotonated amine groups at pH = 10.5 (20).

In a recent EXAFS study (data limit k_{max} = 11 Å^{-1}) of the complexes formed in a dilute mercury(II)–glutathione frozen glass at pH 7.5, formation of a $(GS)_2$-Hg···Hg-$(GS)_2$ dimer in aqueous solution was proposed for the first time, with two Hg–S bond distances of 2.334(4) Å and a Hg···Hg interaction at 2.884(6) Å. It was suggested that "this Hg species could be implicated in the mammalian toxicology of Hg^{2+}" (34). However, in the current study, EXAFS spectra were obtained for solutions **A1** and **A2** at room temperature in a wide *k*-range (up to 14.5 Å^{-1}) and no such Hg···Hg scattering contribution could be observed (Figure S-4). In a survey of the Cambridge Structural Database (CSD, version 5.31, Nov. 2009) (35), we found dimeric complexes (such as COHWEB and DAXRAV) with two bridging thiolate groups, $Hg_2(\mu\text{-}SR)_2$, leading to $Hg^{II}\cdots Hg^{II}$ distances of ~ 3.6 Å (36,37). Single oxygen bridges between two mercury(II) atoms have been found in several crystal structures, leading to $Hg^{II}\cdots Hg^{II}$ distances of 3.5–3.6 Å (38). Mercury(I) forms dimeric Hg_2^{2+} species with direct Hg^I-Hg^I bonds of ~ 2.5 Å (39). Therefore, the proposed dimeric structure with such a short $Hg^{II}\cdots Hg^{II}$ distance as 2.9 Å seems unlikely when considering possible bridging groups.

The ^{199}Hg NMR resonance that appears at −923 ppm for solution **B1** ($C_{Hg(II)}$ ~ 15 mM, C_{GSH} ~ 53 mM) is about ~ +60 ppm deshielded relative to that of **A1** (GSH / Hg(II) = 2.4), but still within the chemical shift range for $Hg(SR)_2$ complexes. For the more concentrated solution **B2** ($C_{Hg(II)}$ ~ 50 mM, C_{GSH} ~ 150 mM), the ^{199}Hg NMR chemical shift deshielded to −786 ppm was considerably broader as compared with **A2** (−960 ppm). Since Hg-S bonds are quite labile in solution, the ^{199}Hg chemical shift is often representative of two or more species in fast exchange (20–22). Three-coordinated aliphatic Hg(II)-thiolate complexes are typically highly deshielded, with ^{199}Hg NMR signals between −79 to −179 ppm (29,31,32,40,41). The chemical shift difference of +137 ppm for solution **B2** versus **B1** implicates a significant difference in the speciation, consistent with the higher free GSH concentration in **B2** that favors formation of some amount of the $[Hg(AH)_3]^{4-}$ complex. Curve-fitting of EXAFS oscillations for solutions **B1** and **B2**, however, resulted in mean Hg-S bond lengths of 2.33 – 2.34 Å, similar to that obtained for **A1** and **A2** (2.325 ± 0.01 Å) implicating that ^{199}Hg NMR is a more sensitive probe of small changes in the Hg(II) speciation.

For the series of solutions **C2** – **F2** ($C_{Hg(II)}$ ~ 50 mM, pH = 7.0), the deshielding of the ^{199}Hg NMR chemical shifts gradually increased relative to **B2** (−786 ppm; C_{GSH} ~ 0.1

M) as the glutathione concentration increased from 0.2 to 0.5 M: **C2** (−657 ppm), **D2** (−606 ppm), **E2** (−483 ppm) and **F2** (−457 ppm). In addition, the mean Hg-S bond distance obtained from the model fitting of the EXAFS spectra increased from 2.34 Å (**B2**) to 2.39 ± 0.02 Å (**F2**), accompanied with a corresponding substantial increase in the disorder parameter (σ^2) from 0.0051 Å^2 to 0.0081 ± 0.0010 Å^2 (Table 3), indicating a wider distribution of the Hg-S distances. Also, for the solutions **C1** – **F1** with GSH / Hg(II) ratios increasing from 4.7 to 11.8 for $C_{Hg(II)}$ ~17 mM, the EXAFS data analyses show a gradual increase in the mean Hg-S bond length from 2.33 to 2.37 ± 0.02 Å, while the disorder parameter (σ^2) for the Hg-S path increases from 0.0049 (**C1**) to 0.0084 (**F1**) ± 0.0010 Å^2.

For both series of solutions, the increase in the Hg-S bond distance, and also in the σ^2 value that represents a large variation around the mean Hg-S distance, especially for solutions **F1** and **F2**, can be attributed to the formation of a significant amount of the $[Hg(AH)_3]^{4-}$ complex at increasing ligand concentration. Since the Hg-S distances differ significantly in the $[Hg(AH)_2]^{2-}$ and $[Hg(AH)_3]^{4-}$ complexes, their corresponding EXAFS oscillations interfere and reduce the amplitude of the EXAFS spectra for solutions **F1** and **F2** in comparison with **A1** and **A2**, and also their Fourier transforms (Figure S-5). Furthermore, a ^{199}Hg resonance could not be detected for the dilute solutions **C1** – **F1** due to chemical exchange broadening in the mixture of HgS_2 and HgS_3 complexes. The presence of *tris*-thiolate complexes was further confirmed by the ESI-MS of solution **F1** (Figure 4).

Speciation of Hg(II)-GSH complexes using PCA of EXAFS spectra

Principal component analysis applied on the nine experimental EXAFS spectra obtained for solutions **C1**–**F1** and **B2**–**F2** showed the presence of two major Hg(II) species (Figure S-1 and Table S1). To quantify the relative proportion of $[Hg(AH)_2]^{2-}$ and $[Hg(AH)_3]^{4-}$ complexes formed in the Hg(II)-GSH solutions **B1** – **F1** at pH = 7.0, the experimental EXAFS spectra were fitted with a linear combination of model oscillations representing these two species. Solution **A1** was assumed to contain 100 % of the $[Hg(AH)_2]^{2-}$ complex, and the fitted curve from the least squares model fitting was used in the linear combinations. The model oscillation for the $[Hg(AH)_3]^{4-}$ complex that gave the best fit to the experimental EXAFS spectra was obtained for 3 Hg-S distances at 2.42 Å, σ^2 = 0.0060 Å^2, S_0^2 = 1.0 and ΔE_0 = 9.0. To summarize, the Hg-S distances 2.325 Å (σ^2 = 0.0040 Å) for $[Hg(AH)_2]^{2-}$, and 2.42 Å (σ^2 = 0.0060 Å) for $[Hg(AH)_3]^{4-}$, resulted in the best linear combination fits. The results are provided in Table 4 (see Figure S-2).

The $[Hg(AH)_2]^{2-}$ complex predominates (87–100 %, Table 4) for solutions **A1**–**C1** where the free GSH concentration is less than ~0.04 M. Even though the least-squares refinement procedure resulted in quite similar mean Hg-S distances of 2.33 ± 0.02 Å for solutions **A1** – **C1** (Table 2), the linear combination fitting indicates that a minor amount of the $[Hg(AH)_3]^{4-}$ complex is present in **B1** and **C1** (~5–13 %). For solutions **D1** and **F1**, with free GSH concentrations of ~0.06 and 0.16 M, the amount of the $[Hg(AH)_3]^{4-}$ complex increases to about 21 and 48%, respectively.

The relative amounts of $[Hg(AH)_2]^{2-}$ and $[Hg(AH)_3]^{4-}$ complexes formed in the Hg(II)-GSH solutions **B2** – **F2** at pH = 7.0 were quantified by a similar method (Figure S-3, Table 4), assuming that solution **A2** contains 100 % of the $[Hg(AH)_2]^{2-}$ complex. The results from the linear combination fitting show somewhat higher amounts (~20–30 %) of the $[Hg(AH)_3]^{4-}$ complex in the solutions **B2** – **F2** (free GSH concentration ~0.04 – 0.35 M, $C_{Hg(II)}$ ~50 mM) than in the solutions **B1** – **F1** (free GSH concentration ~ 0.02 – 0.16 M, $C_{Hg(II)}$ ~17 mM) for similar ratios of GSH/Hg(II). Solution **B2** with free GSH concentration ~0.04 M has ~78 % $[Hg(AH)_2]^{2-}$ and ~22 % $[Hg(AH)_3]^{4-}$ complexes, consistent with the deshielded ^{199}Hg chemical shift −786 ppm, while the more dilute solution **B1** with similar ratio GSH/Hg(II) = 3.5 (free GSH concentration ~0.02 M), only has ~5 % of the

$[Hg(AH)_3]^{4-}$ complex and the ^{199}Hg chemical shift −923 ppm (Figure 1). In the concentrated solutions **C2** and **D2** with GSH/Hg(II) = 4.0 and 5.0 (free GSH concentration ~0.08 M and ~0.13 M, respectively), approximately 40–45 % of the total Hg(II) amount is present as the three-coordinated complex. Also in solution **F1** ($C_{Hg(II)}$ ~17 mM, GSH/Hg(II) = 11.8) with lower Hg(II) concentration and similar free GSH concentration (~0.16 M) as **D2**, almost half is present as the $[Hg(AH)_3]^{4-}$ complex. With large excess of free GSH (> 0.35 M) as for solution **F2** (C_{GSH} = 500 mM, $C_{Hg(II)}$ ~50 mM), the $[Hg(AH)_3]^{4-}$ complex predominates (~70 % of the Hg(II) species). Figure 5 visualizes the percentage of the $[Hg(AH)_3]^{4-}$ complex formed in Hg(II)-glutathione solutions **A1** – **F1**, and **A2** – **F2** at pH = 7.0, as obtained from a linear combination fitting of HgS_2 and HgS_3 models to their EXAFS spectra (Table 4). For both series approximately equal concentrations of HgS_2 and HgS_3 species are reached for an excess amount of free GSH of ~0.17 M at pH 7.0.

The relative proportions of HgS_2 and HgS_3 species obtained by the fitting of the EXAFS data (Table 4) are in qualitative agreement with distribution diagrams of the major Hg(II)-glutathione species *vs*. pH, calculated by means of the available stability constants from the literature (see Appendix I and Refs. (8,19). Such calculated diagrams confirm that the $[Hg(AH)_2]^{2-}$ and $[Hg(AH)_3]^{4-}$ complexes are the major Hg(II)-GSH species at neutral pH, with the glutathione amine group still being protonated. However, the literature values gave slightly different ratios between the major HgS_2 and HgS_3 species (at pH = 7.0 $[Hg(AH)_2]^{2-}$ and $[Hg(AH)_3]^{4-}$ complexes) than those obtained experimentally for the solutions in the current study. Assuming that the reported stability constant well characterizes the stable $[Hg(AH)_2]^{2-}$ complex, we therefore adjusted the stability constant of the $[Hg(AH)_3]^{4-}$ complex to obtain calculated $[Hg(AH)_2]^{2-}$: $[Hg(AH)_3]^{4-}$ ratios close to those in Table 4 (see Appendix I; Figure S-6a). The formation constant for the $[Hg(AH)_3]^{4-}$ complex, defined as $Hg^{2+} + 3A^{3-} + 3H^+ \leftrightarrow HgA_3H_3^{4-}$, with the reported value log β_7 = 72.75 (19), then attained the value log β_7 72.22 for both series of solutions in Table 4. Since the deprotonation of the amine group of the HgS_3 species is independent of the Hg-S coordination, the formation constants for all HgS_3 species were shifted with the same amount, −0.53 logarithmic units (see Appendix I). Fraction diagrams in Figures 6,S-7a and S-7b, calculated using the adjusted stability constants, demonstrate the distribution of Hg(II)-glutathione complexes *vs*. pH for solutions **B1**, **B2**, **F1** and **F2**. The calculated distribution of complexes for solution **F2** shows that the amino groups of the $[Hg(AH)_3]^{4-}$ complex has started to deprotonate at pH = 7.0 with about 3% of the mercury(II) amount present in the $[Hg(AH)_2(A)]^{5-}$ complex (Figure 6). The stability constant for the formation of the HgA_4^{10-} complex could be estimated to log β_{10} = 44.8 for $Hg^{2+} + 4A^{3-} \leftrightarrow HgA_4^{10-}$ (which then also includes possible contributions from deprotonated HgS_4 species) from the previously determined distributions of HgS_2, HgS_3 and HgS_4 species at pH = 10.5 (20); see below and Appendix 1, Figure S-6b.

Effect of pH on Hg(II)-GSH speciation

In our previous EXAFS study of Hg(II)-GSH complex formation in alkaline aqueous solution (pH = 10.5, $C_{Hg(II)}$ ~18 mM), the deprotonated $[Hg(A)_2]^{4-}$, $[Hg(A)_3]^{7-}$ and $[Hg(A)_4]^{10-}$ complexes were characterized. By increasing the C_{GSH} from 40 mM to 200 mM in the alkaline solutions, the average Hg-S distance obtained from EXAFS spectra elongated from 2.315 to 2.44 Å (20), while for the neutral solutions **A1** – **F1** with similar chemical composition the variation of the mean Hg-S distances was smaller, from 2.325 to 2.37 Å. Furthermore, for the alkaline solutions containing $C_{Hg(II)}$ ~18 mM and excess glutathione (C_{GSH} = 160 – 200 mM), a deshielded ^{199}Hg resonance at ~ −300 ppm could be detected, which is due to the predominating $[Hg(A)_3]^{7-}$ and the minor (20–30%) $[Hg(A)_4]^{10-}$ species (see Figure 7) (20). The formation of HgS_3 and HgS_4 complexes at pH = 10.5 (GSH/Hg(II) > 11), is promoted by the deprotonation of the cysteinyl thiol group to

thiolate in alkaline solution, which occurs between pH 9 to 10 according to sulfur K-edge XANES measurements (42). At pH = 7.0 the thiol group in free GSH is only deprotonated to a minor extent. Thus, even at high glutathione concentration as in the currently studied solutions, the thiolate concentration is not sufficient (Figure S-7c) to promote a detectable amount of a four coordinated HgS_4 species, which presumably would be the $[Hg(AH)_4]^{6-}$ complex in neutral solutions.

Conclusions

The Hg L_{III}-edge EXAFS and ^{199}Hg NMR results for two series of Hg(II)-GSH solutions with $C_{Hg(II)}$ = 17 and 50 mM at pH 7.0 show that $[Hg(AH)_2]^{2-}$ and $[Hg(AH)_3]^{4-}$ complexes (Scheme 2) form at physiological pH in aqueous solutions. The $[Hg(AH)_2]^{2-}$ complex with linear S-Hg-S coordination and the Hg-S bond distances 2.325 ± 0.01 Å and the ^{199}Hg NMR resonance at −984 ppm, dominates except at high excess of glutathione. In solutions with free glutathione concentration higher than ~0.17 M at pH = 7.0 the $[Hg(AH)_3]^{4-}$ complex with trigonal HgS_3 coordination and an average Hg-S bond distance of 2.42 ± 0.02 Å, dominates. *Tris*-glutathionyl Hg(II) complexes were also detected by ESI-MS. For a corresponding series of alkaline solutions (pH = 10.5), for which our previous results showed that also HgS_4 species formed (20), we have estimated a formation constant of log β = 44.8 ($Hg^{2+} + 4A^{3-} \leftrightarrow HgA_4^{10-}$) for the $[Hg(A)_4]^{10-}$ complex with deprotonated amino groups. However, at pH 7.0 the four-coordinated $[Hg(AH)_4]^{6-}$ complex does not form because of the highly protonated thiol groups in the free GSH ligands (42). For the series of solutions containing $C_{Hg(II)}$ ~50 mM and GSH/Hg(II) = 3.0–10.0 at pH 7.0, a somewhat higher proportion of the $[Hg(AH)_3]^{4-}$ complex is formed as compared with solutions containing $C_{Hg(II)}$ ~17 mM despite similar ligand to metal mole ratios, because of the lower concentration of free GSH.

Following Cheesman and coworkers, the equilibrium properties of the mercury(II) complexes *in vivo* are predicted, *i.e.* for the total glutathione concentration 2.2 mM and the pH = 7.4, as in human erythrocytes (18). Calculations performed for Hg(II) concentrations from 0 to 1 mM with our adjusted stability constants show that at low Hg(II) concentrations the $[Hg(AH)_2]^{2-}$ complex dominates at pH = 7.4, and that the highest proportion of the $[Hg(AH)_3]^{4-}$ complex, about 3%, occurs in media with $C_{Hg(II)} < \sim 0.1$ mM (Figure S-8a), which is less than that previously proposed by Cheesman et al (18) (~11%). The percentage is slightly reduced at higher Hg(II)-concentration because of the lower free GSH concentration. About 2% of the total Hg(II) amount is present as the deprotonated HgS_2 complex $[Hg(AH)(A)]^{3-}$ at pH 7.4 (Figure S-8).

Synopsis

Combined ^{199}Hg NMR, Hg L_{III}-edge X-ray absorption and mass spectroscopic studies reveal the amount of two and three-coordinated Hg(II)-glutathione complexes, with the mean Hg-S bond distances 2.325 and 2.42 ± 0.02 Å, respectively, that form in aqueous solution at pH 7.0.

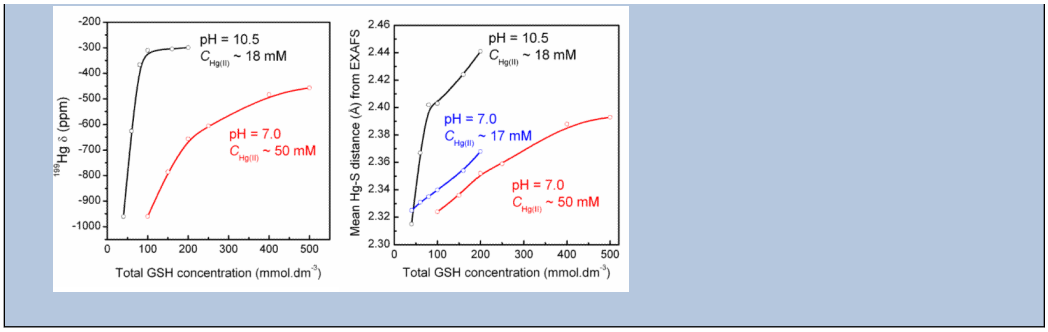

Supplementary Material

Refer to Web version on PubMed Central for supplementary material.

Acknowledgments

We thank Mrs. Qiao Wu for her skillful assistance with the ESI-MS measurements. We are grateful to Professor Jürgen Gailer and Shawn Manley for ICP analyses. X-ray absorption measurements were carried out at the Stanford Synchrotron Radiation Laboratory, SSRL, (proposal No. 2848), a US national user facility operated by Stanford University on behalf of the US Department of Energy, Office of Basic Energy Sciences. The SSRL Structural Molecular Biology Program is supported by the Department of Energy, Office of Biological and Environmental Research, and by the National Institutes of Health, National Center for Research Resources, Biomedical Technology Program. We are grateful to the National Science and Engineering Research Council (NSERC) of Canada, the Canadian Foundation for Innovation (CFI) and the Province of Alberta (Department of Innovation and Science) for their financial support. F.J. is a recipient of a NSERC University Faculty Award (UFA).

References

(1). George GN, Singh SP, Hoover J, Pickering IJ. The chemical forms of mercury in aged and fresh dental amalgam surfaces. Chem Res Toxicol. 2009; 22:1761–1764. [PubMed: 19842619]

(2). Korbas M, Blechinger SR, Krone PH, Pickering IJ, George GN. Localizing organomercury uptake and accumulation in zebrafish larvae at the tissue and cellular level. Proc Natl Acad Sci U S A. 2008; 105:12108–12112. [PubMed: 18719123]

(3). George GN, Singh SP, Myers GJ, Watson GE, Pickering IJ. The chemical forms of mercury in human hair: a study using X-ray absorption spectroscopy. J Biol Inorg Chem. 2010; 15:709–715. [PubMed: 20225071]

(4). Clarkson TW. The three modern faces of mercury. Environ Health Perspect. 2002; 110(Suppl 1): 11–23. [PubMed: 11834460]

(5). Clarkson TW, Magos L. The toxicology of mercury and its chemical compounds. Crit Rev Toxicol. 2006; 36:609–662. [PubMed: 16973445]

(6). Kapoor RC, Doughty G, Gorin G. The Reaction and Assay of Glutathione with Hg2+ and Alkali. Biochim Biophys Acta. 1965; 100:376–383. [PubMed: 14347934]

(7). Oram PD, Fang X, Fernando Q, Letkeman P, Letkeman D. The formation of constants of mercury(II)--glutathione complexes. Chem Res Toxicol. 1996; 9:709–712. [PubMed: 8831814]

(8). Stricks W, Kolthoff IM. Reactions between Mercuric Mercury and Cysteine and Glutathione. Apparent Dissociation Constants, Heats and Entropies of Formation of Various Forms of Mercuric Mercapto-Cysteine and -Glutathione. J. Am. Chem. Soc. 1953; 75:5673–5681.

(9). Neville GA, Drakenberg T. Acta Chem. Scand. B. 1974; 28:473–477. [PubMed: 4853164]

(10). Rabenstein DL, Isab AA. Biochim. Biophys. Acta. 1982; 721:374–384. [PubMed: 7159599]

(11). Sudmeier JL, Birge RR, Perkins TG. J. Magn. Reson. 1978; 30:491–496.

(12). Burford N, Eelman MD, Groom K. J. Inorg. Biochem. 2005; 99:1992–1997. [PubMed: 16084595]

(13). Rubino FM, Verduci C, Giampiccolo R, Pulvirenti S, Brambilla G, Colombi A. J. Am. Soc. Mass Spectrom. 2004; 15:288–300. [PubMed: 14998531]

(14). Krupp EM, Milne BF, Mestrot A, Meharg AA, Feldmann J. Anal. Bioanal. Chem. 2008; 390:1753–1764. [PubMed: 18297471]

(15). Rubino FM, Pitton M, Brambilla G, Colombi A. J. Mass Spectrom. 2006; 41:1578–1593. [PubMed: 17136764]

(16). Fuhr BJ, Rabenstein DL. J. Am. Chem. Soc. 1973; 95:6944–6950. [PubMed: 4784285]

(17). Katōno Y, Inoue Y, Chûjô R. Polymer J. 1977; 9:471–478.

(18). Cheesman BV, Arnold AP, Rabenstein DL. Nuclear magnetic resonance studies of the solution chemistry of metal complexes. 25. Hg(thiol)3 complexes and HG(II)-thiol ligand exchange kinetics. J. Am. Chem. Soc. 1988; 110:6359–6364.

(19). Shoukry MM, Cheesman BV, Rabenstein DL. Polarimetric and nuclear magnetic resonance studies of the complexation of mercury by thiols. Can. J. Chem. 1988; 66:3184–3189.

(20). Mah V, Jalilehvand F. Mercury(II) complex formation with glutathione in alkaline aqueous solution. J. Biol. Inorg. Chem. 2008; 13:541–553. [PubMed: 18224359]

(21). Jalilehvand F, Leung BO, Izadifard M, Damian E. Mercury(II) Cysteine Complexes in Alkaline Aqueous Solution. Inorg. Chem. 2006; 45:66–73. [PubMed: 16390041]

(22). Leung BO, Jalilehvand F, Mah V. Mercury(II) penicillamine complex formation in alkaline aqueous solution. Dalton Trans. 2007:4666–4674. [PubMed: 17940647]

(23). Klose G, Volke F, Peinel G, Knobloch G. ^{199}Hg NMR of Aqueous Solutions of Inorganic Mercury salts. Chemical shifts of $HgCl_n^{2-n}$ with n = 0–4. Magn. Reson. Chem. 1993; 31:548–551.

(24). George, GN.; Geroge, SJ.; Pickering, IJ. EXAFSPAK. Stanford Synchrotron Radiation Lightsource (SSRL); Menlo Park, CA: 2001.

(25). Ressler T. *WinXAS*: a Program for X-ray Absorption Spectroscopy Data Analysis under MS-Windows. J. Synchrotron Rad. 1998; 5:118–122.

(26). Ankudinov AL, Rehr JJ. Relativistic calculations of spin-dependent x-ray-absorption spectra. Phys. Rev. B. 1997; 56:R1712.

(27). Zabinsky SI, Rehr JJ, Ankudinov A, Albers RC, Eller MJ. Multiple-scattering calculations of x-ray-absorption spectra. Phys. Rev. B. 1995; 52:2995.

(28). Kim C-H, Parkin S, Bharara M, Atwood D. Linear coordination of Hg(II) by cysteamine. Polyhedron. 2002; 21:225–228.

(29). Bowmaker GA, Harris RK, Oh S-W. Solid-state NMR spectroscopy of mercury compounds. Coord. Chem. Rev. 1997; 167:49–94.

(30). Natan MJ, Millikan CF, Wright JG, O'Halloran TV. Solid-state mercury-199 nuclear magnetic resonance as a probe of coordination number and geometry in Hg(II) complexes. J. Am. Chem. Soc. 1990; 112:3255–3257.

(31). Utschig LM, Bryson JW, O'Halloran TV. Mercury-199 NMR of the metal receptor site in MerR and its protein-DNA complex. Science. 1995; 268:380–385. [PubMed: 7716541]

(32). Wright JG, Natan MJ, MacDonnell FM, Ralston DM, O'Halloran TV. Prog. Inorg. Chem. 1990; 38:323–412.

(33). Manceau A, Nagy KL. Relationships between Hg(II)-S bond distance and Hg(II) coordination in thiolates. Dalton Trans. 2008:1421–1425. [PubMed: 18322620]

(34). Percy AJ, Korbas M, George GN, Gailer J. J. Chromatogr. A. 2007; 1156:331–339. [PubMed: 17222858]

(35). Allen FH. The Cambridge Structural Database: a quarter of a million crystal structures and rising. Acta Cryst. B. 2002; B58:380–388. [PubMed: 12037359]

(36). Bowmaker GA, Dance IG, Dobson BC, Rogers DA. Syntheses and Vibrational-Spectra of Some Tris(Alkanethiolato)Mercurate(Ii) Complexes, and Crystal-Structure of the Hexakis(Methanethiolato)Dimercurate(Ii) Dianion. Australian Journal of Chemistry. 1984; 37:1607–1618.

(37). Henkel G, Betz P, Krebs B. [Hg3(Sch2ch2s)4]2- and ([Hg2(Sch2ch2s)3]2-)-Normal - Examples of Trinuclear and Quasi-Isolated Binuclear Polymeric Mercury Thiolate Anions. Journal of the Chemical Society-Chemical Communications. 1985:1498–1499.

(38). Sandström M. An X-ray Diffraction and Raman Study of Chloride, Bromide and Iodide Complexes of Mercury(II) in Dimethyl Sulfoxide Solution and of Mercury(II) Chloride in Methanol Solution. Acta Chem. Scand. A. 1978; 32:627–641.

(39). Rosdahl J, Persson I, Kloo L, Ståhl K. On the solvation of the mercury(I) ion. A structural, vibration spectroscopic and quantum chemical study. Inorg. Chim. Acta. 2004; 357:2624–2634.

(40). Dieckmann GR, McRorie DK, Tierney DL, Utschig LM, Singer CP, O'Halloran TV, Penner-Hahn JE, DeGrado WF, Pecoraro VL. De Novo Design of Mercury-Binding Two- and Three-Helical Bundles. J. Am. Chem. Soc. 1997; 119:6195–6196.

(41). Matzapetakis M, Farrer BT, Weng T-C, Hemmingsen L, Penner-Hahn JE, Pecoraro VL. Comparison of the Binding of Cadmium(II), Mercury(II), and Arsenic(III) to the de Novo Designed Peptides TRI L12C and TRI L16C. J. Am. Chem. Soc. 2002; 124:8042–8054. [PubMed: 12095348]

(42). Risberg ED, Jalilehvand F, Leung BO, Pettersson LGM, Sandstrom M. Theoretical and experimental sulfur K-edge X-ray absorption spectroscopic study of cysteine, cystine, homocysteine, penicillamine, methionine and methionine sulfoxide. Dalton Trans. 2009:3542–3558. [PubMed: 19381417]

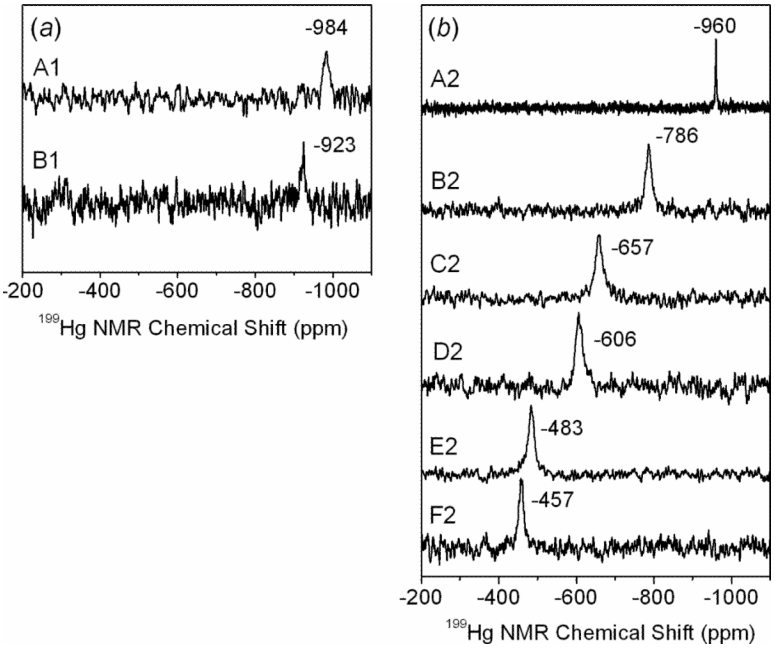

Figure 1.

^{199}Hg NMR spectra for the Hg(II)-GSH solutions at pH = 7.0: (*a*) **A1** and **B1** ($C_{Hg(II)}$ ~ 15 mM, GSH/Hg(II) mole ratios = 2.4 and 3,5, respectively), (*b*) **A2** – **F2** ($C_{Hg(II)}$ ~50 mM, GSH/Hg(II) mole ratios = 2.0–10.0).

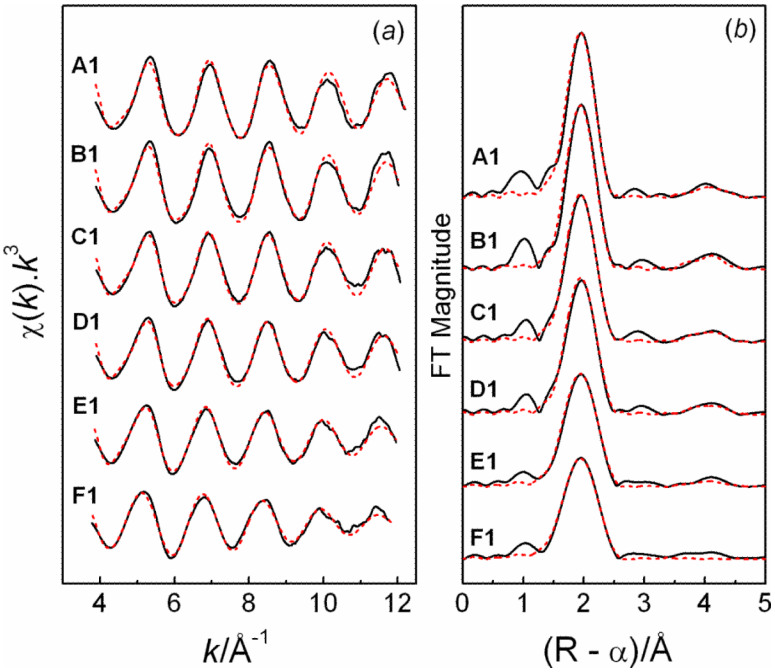

Figure 2.
(a) Hg L_{III}-edge EXAFS spectra for the Hg(II)-GSH solutions with GSH/Hg(II) mole ratios 2.4 (**A1**), 3.5 (**B1**), 4.7 (**C1**), 5.9 (**D1**), 9.4 (**E1**), and 11.8 (**F1**), $C_{Hg(II)}$ ~17 mM, pH = 7.0 (— experimental data; --- model). Structural parameters are listed in Table 2. (b) Corresponding Fourier transforms.

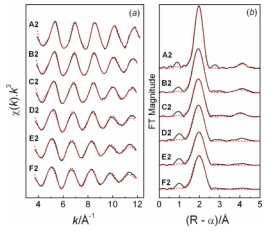

Figure 3.

(a) Hg L_{III}-edge EXAFS spectra for Hg(II)-GSH solutions with $C_{Hg(II)}$ ~50 mM and GSH/Hg(II) mole ratios 2.0 (**A2**), 3.0 (**B2**), 4.0 (**C2**), 5.0 (**D2**), 8.0 (**E2**), 10.0 (**F2**), at pH = 7.0 (— experimental data; --- model). Structural parameters are listed in Table 3. (b) Corresponding Fourier transforms.

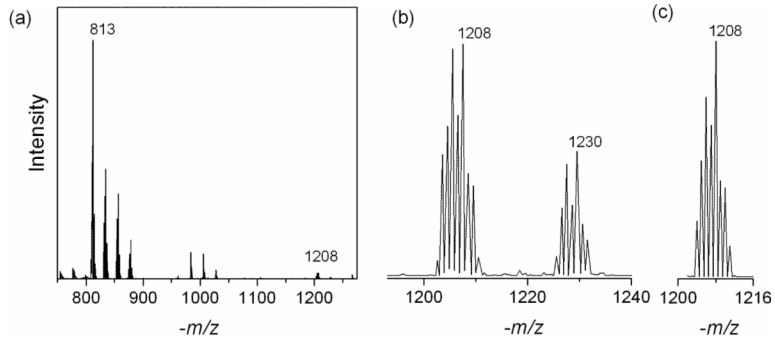

Figure 4.

(a) ESI-MS measured in the negative ion mode for solution **F1** with GSH/Hg(II) = 11.8 at pH = 7.0; (b) expanded region showing peaks labeled −*m/z* 1208 and 1230 assigned as the most abundant ^{202}Hg isotopomers of the $[Na_4Hg(AH)_2(A)]^-$ and $[Na_5Hg(AH)(A)_2]^-$ species. (c) Calculated isotopic distribution for $[Na_4Hg(AH)_2(A)]^-$.

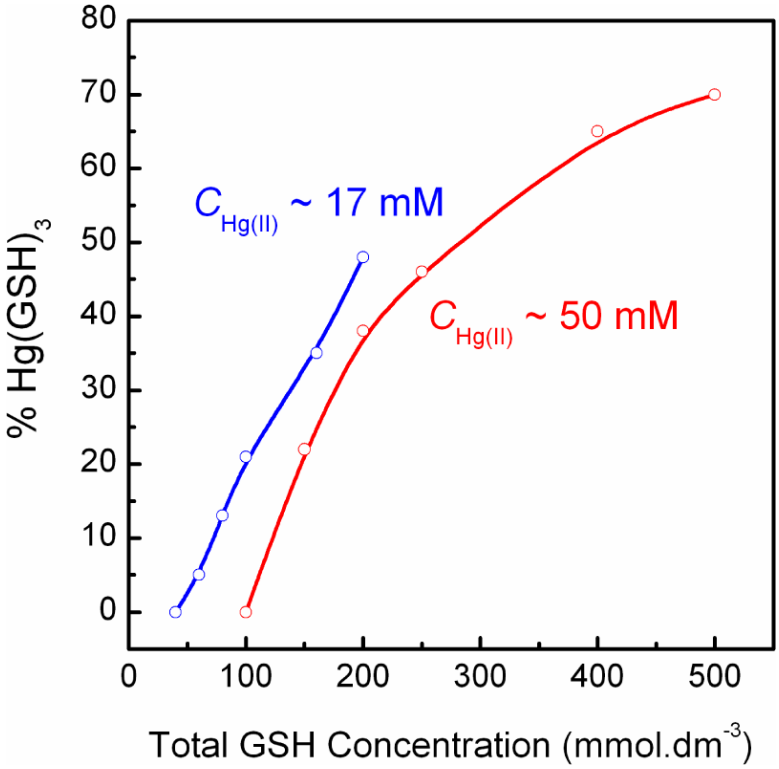

Figure 5.
Percentage of the *tris*-glutathionyl Hg(II) complex $[Hg(AH)_3]^{4-}$ in solutions **A1**–**F1** ($C_{Hg(II)}$ ~ 17 mM) and **A2**–**F2** ($C_{Hg(II)}$ ~ 50 mM) at pH 7.0, as obtained from fitting linear combinations of HgS_2 and HgS_3 EXAFS oscillations to their spectra (Table 4).

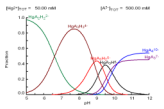

Figure 6.
Fraction diagram showing the distribution of major Hg(II) complexes *vs*. pH for an aqueous solution containing $C_{Hg(II)}$ = 0.050 M and C_{GSH} = 0.5 M, as in solution **F2**, calculated according to the adjusted formation constants (see Appendix I, Supporting Information).

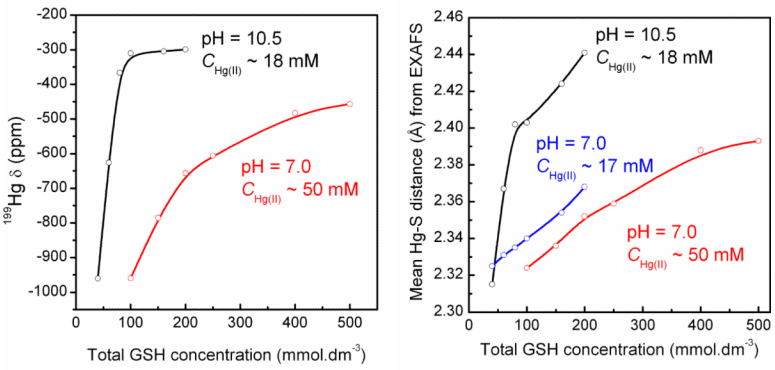

Figure 7.

(*left*) Variation of the ^{199}Hg NMR chemical shift (ppm) with the total glutathione concentration for two series of Hg(II)-GSH solutions at neutral ($C_{Hg(II)}$ = 50 mM) and alkaline pH ($C_{Hg(II)}$ = 18 mM); (*right*) Variation of the mean Hg-S bond distance obtained from EXAFS spectra of these solutions (see Tables 2 and 3) (20).

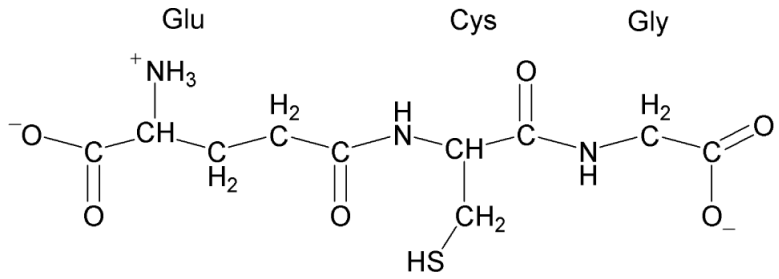

Scheme 1.
The major form of glutathione at pH = 7.0 (AH_2^-).

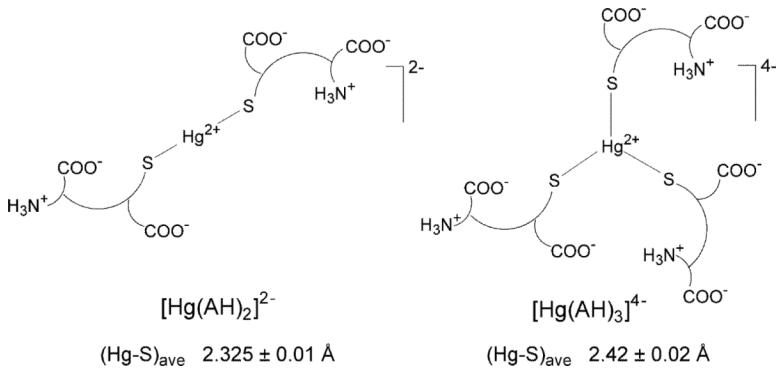

Scheme 2.

Proposed structures for the major Hg(II)- glutathione complexes at pH = 7.0.

Table 1

Composition of the Hg(II)-GSH Solutions Studied at pH = 7.0.

Solution	$C_{GSH}/C_{Hg(II)}$	$C_{Hg(II)}$ (mM)	C_{GSH} (mM)
A1	2.4	17[a]	40
B1	3.5	17[a]	60
C1	4.7	17	80
D1	5.9	17	100
E1	9.4	17	160
F1	11.8	17	200
A2	2.0	50	100
B2	3.0	50	150
C2	4.0	50	200
D2	5.0	50	250
E2	8.0	50	400
F2	10.0	50	500

[a] For ^{199}Hg NMR measurements, 10% (v/v) D_2O was added to these solutions, reducing $C_{Hg(II)}$ to ~15 mM.

Table 2

Structural Parameters Derived from EXAFS Least-Squares Curve Fitting for the Hg(II)-GSH Solutions **A1 – E1** at pH = 7.0 ($C_{Hg(II)}$ ~17 mM; see Figure 2).[a]

Solution (GSH/Hg(II))	Hg-S			Additional contributions					
	N	*R* (Å)	σ^2 (Å^2)		N[b]	*R* (Å)	σ^2 (Å^2)	ΔE_0 (eV)	R[c]
A1 (2.4)	2.1	2.325	0.0041	S-Hg-S	2.1	4.66	0.0104	10.6	18.8
B1 (3.5)	2.0	2.331	0.0034	S-Hg-S	2.0	4.65	0.0071	10.7	19.0
C1 (4.7)	2.1	2.335	0.0049	S-Hg-S	2.1	4.65	0.0118	10.3	14.2
D1 (5.9)	2.1	2.340	0.0053	S-Hg-S	2.1	4.65	0.0125	9.8	15.0
E1 (9.4)	2.2	2.354	0.0063	S-Hg-S	2.2	4.65	0.0195	9.6	17.4
F1 (11.8)	2.5	2.368	0.0084					9.1	18.2

[a] Fitting *k*-range = 3.9 – 12.0 Å^{-1}; S_0^2 = 1.0; estimated error limits: *N* ± 20 %, *R* ± 0.02 Å, σ^2±2 0.001 Å^2;

[b] Correlated to the coordination number *N* of Hg-S path.

[c] The residual (%) from the least-squares curve fitting is defined as:

$$\frac{\sum_{i=1}^{N} \left| y_{\mathrm{exp}^{(i)}} - y_{\mathrm{theo}^{(i)}} \right|}{\sum_{i=1}^{N} \left| y_{\mathrm{exp}^{(i)}} \right|} \times 100$$

where y_{exp} and y_{theo} are experimental and theoretical data points, respectively.

Table 3

Structural Parameters Derived from EXAFS Least-Squares Curve Fitting for the Hg(II)-GSH Solutions **A2 – F2** at pH = 7.0 ($C_{Hg(II)}$ ~50 mM; see Figure 3).[a]

Solution (GSH/Hg(II))	Hg-S			Additional contributions					
	N	R (Å)	σ (Å^2)		N[b]	R (Å)	σ (Å^2)	ΔE_0 (eV)	R[c]
A2 (2.0)	2.1	2.324	0.0035	S-Hg-S	2.1	4.66	0.0078	10.7	12.3
B2 (3.0)	2.2	2.336	0.0051	S-Hg-S	2.2	4.64	0.0122	9.4	13.1
C2 (4.0)	2.2	2.352	0.0063	S-Hg-S	2.2	4.63	0.0120	8.9	16.9
D2 (5.0)	2.4	2.359	0.0075					8.4	21.1
E2 (8.0)	2.6	2.388	0.0086					8.9	19.2
F2 (10.0)	2.5	2.393	0.0081					8.9	20.1

[a] Fitting *k*-range = 3.7 – 12.0 Å^{-1}; S_0^2 = 1.0; estimated error limits: *N* ± 20 %, *R* ± 0.02 Å, σ^2 ± 0.001 Å^2;

[b] Correlated to the coordination number *N* of Hg-S path.

[c] Residual.

Table 4

Percentage of $[Hg(AH)_2]^{2-}$ and $[Hg(AH)_3]^{4-}$ Complexes Obtained by Linear Combination Fitting of EXAFS data for the Hg(II)-GSH Solutions **A1 - F1** and **A2–F2**.[a]

Solution (GSH/Hg^{2+})	C_{GSH} (mM)	$\delta_{Hg(II)}$ (ppm)	% HgS_2	% HgS_3
A1 (2.4)	40	−984	100	0
B1 (3.5)	60	−923	95	5
C1 (4.7)	80		87	13
D1 (5.9)	100		79	21
E1 (9.4)	160		65	35
F1 (11.8)	200		52	48
A2 (2.0)	100	−960	100	0
B2 (3.0)	150	−786	78	22
C2 (4.0)	200	−657	62	38
D2 (5.0)	250	−606	54	46
E2 (8.0)	400	−483	35	65
F2 (10.0)	500	−457	30	70

[a]The percentages shown are for the best fits with Hg-S bond distances 2.325 Å for $[Hg(AH)_2]^{2-}$ and 2.42 Å for $[Hg(AH)_3]^{4-}$ complexes. The estimated error is ±15 %.